**Supplementary tables and figures**

**Table S1:** RNAseq data whole tumors

**Table S2:** RNAseq data, isolated CAFs

**Table S3:** List of antibodies

| Antibody | Cat. No. | Vendor | Panel |
|---|---|---|---|
| PE anti-human CD140a (PDGFRα) | 323505 | Biolegend | General |
| PE/Cy7 anti-mouse CD19 | 115520 | Biolegend | Lymphoid |
| Brilliant Violet 421™ anti-mouse CD 274 (B7-H1, PD-L1) | 124315 | Biolegend | General |
| FITC anti-mouse CD31 | 102406 | Biolegend | General |
| PE Rat 1gG2a, k isotype control | 400508 | Biolegend | General |
| FAP Biotinylated Antibody | BAF3715 | R&D Systems/Bio-Techne | General |
| FITC anti-mouse CD11c | 117306 | Biolegend | Myeloid |
| Brilliant Violet 421™ anti-mouse CD4 | 100438 | Biolegend | Lymphoid |
| APC/Cy7 anti-mouse NK1.1 | 108724 | Biolegend | Lymphoid |
| APC anti-mouse CD8a | 100712 | Biolegend | Lymphoid |
| PE anti-mouse CD206 (MMR) | 141705 | Biolegend | Myeloid |
| FITC anti-mouse CD3 | 100204 | Biolegend | Lymphoid |
| PE/Cy7 anti-mouse CD45 | 103114 | Biolegend | General |
| Brilliant Violet 421™ anti-mouse CD103 | 121422 | Biolegend | Myeloid |
| PE anti-mouse CD279 (PD-1) | 109103 | Biolegend | Lymphoid |
| PerCP/Cy5.5 anti-mouse CD25 | 101912 | Biolegend | Lymphoid |
| APC/Cy7 anti-mouse Ly-6G | 127623 | Biolegend | Myeloid |
| APC anti-mouse F4/80 | 123116 | Biolegend | Myeloid |
| PE/Cy7 anti-mouse CD11b | 101215 | Biolegend | Myeloid |
| PerCP/Cy5.5 anti-mouse Ly-6C | 128011 | Biolegend | Myeloid |
| Zombie Aqua™ Fixable Viability Kit | 423102 | Biolegend | All panels |
| APC Streptavidin | 405207 | Biolegend | General |

**Table S4:** List of primers used for qRT-PCR

| Gene | Primer name | Sequence (5' - 3') |
|---|---|---|
| *Col1a1* | Col1a1_fw | CTGACTGGAAGAGCGGAGAG |
| | Col1a1_rv | GACGGCTGAGTAGGGAACAC |
| *Mrc2* | Mrc2_fw | CCACAACAGCTGCTACTGGA |
| | Mrc2_rv | AGGGCTGCTGATGGCAAG |
| *Acta2* | Acta2_fw | CATCTTTCATTGGGATGGAGTCAG |
| | Acta2_rv | ACAGGACGTTGTTAGCATAGAGA |
| *Il6* | Il6_fw | GTCTTCTGGAGTACCATAGC |
| | Il6_rv | GTCAGATACCTGACAACAGG |
| *Cxcl12* | Cxcl12_fw | CGGTTCTTCGAGAGCCACAT |
| | Cxcl12_rv | GCCGTGCAACAATCTGAAGG |
| *Tgfb1* | Tgfb1_fw | AGCCCTGTATTCCGTCTCCT |
| | Tgfb1_rv | CTGCTGACCCCCACTGATAC |
| *Arg1* | Arg1_fw | CAGAAGAATGGAAGAGTCAG |
| | Arg1_rv | CAGATATGCAGGGAGTCACC |
| *Cd274* | Cd274_fw | TCACTTGCTACGGGCGTTT |
| | Cd274_rv | CCCAGTACACCACTAACGCA |

**Figure S1**

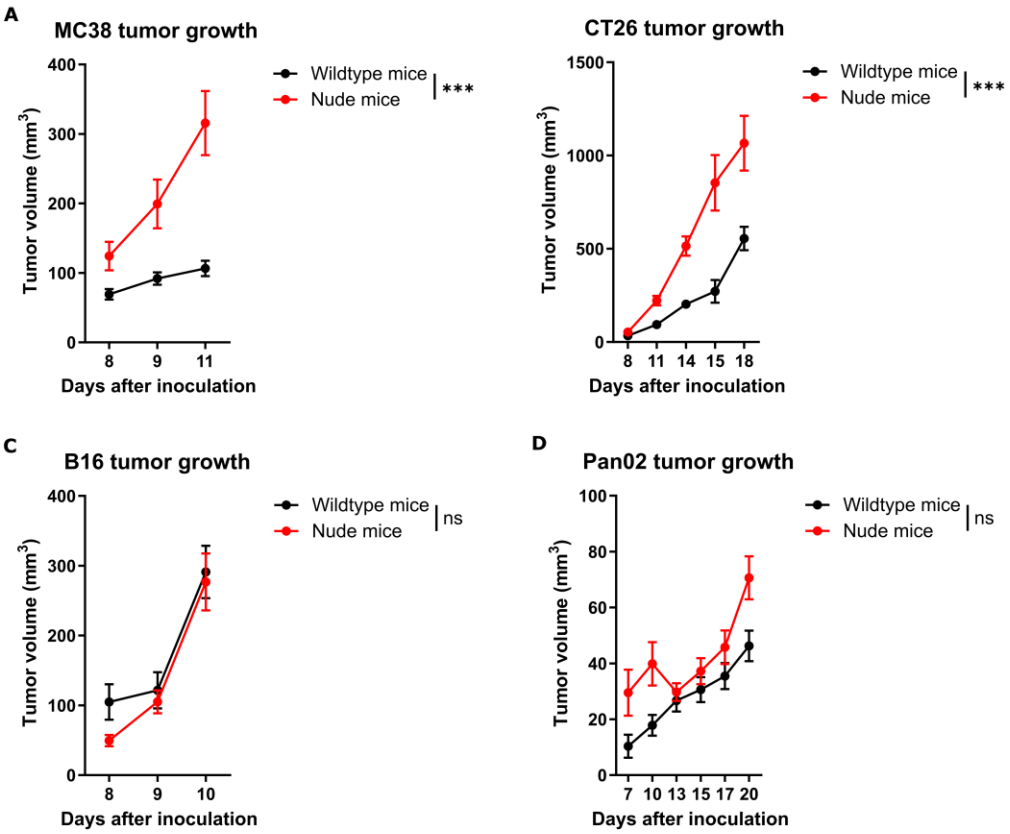


**Figure S1:**

**Tumor growth of the syngeneic murine tumor models MC38, CT26, B16, and Pan02 in wildtype mice (black) and nude mice (red).** A-D) Cancer cells were subcutaneously injected in the flank of C57BL/6 mice (MC38 (A), B16 (C), and Pan02 (D)) or BALB/c mice (CT26 (B)), n = 10-15. Error bars indicate the standard error of the mean (SEM). Statistical analysis was performed by two-way ANOVA with Bonferroni correction, *** = $p \leq 0.001$, ** = $p \leq 0.01$, * = $p \leq 0.05$not significant when $p > 0.05$.

Figure S2

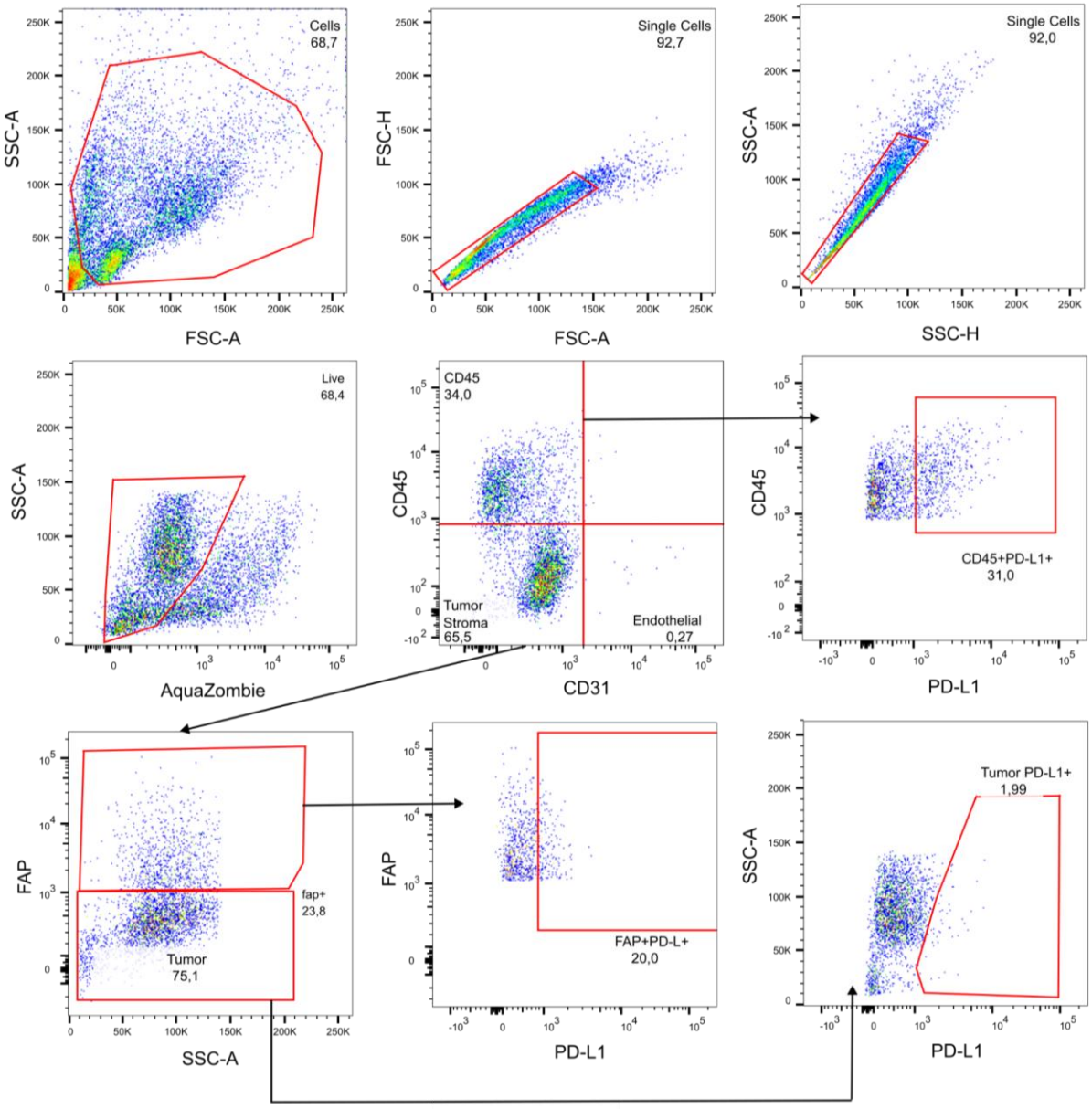


**Figure S2:**

**Gating strategy for general panel.** Representative plots from flow cytometry analysis showing the gating strategy for identification of the indicated cell populations from a single cell suspension of a LL2 tumor. After exclusion of doublets and dead cells (Zombie Aqua-negative), leukocytes ($CD45^+$) and endothelial cells ($CD31^+$) were identified. From the negative population, CAFs ($FAP^+$) and tumor cells ($CD45^-CD31^-FAP^-$) were identified. PD-L1 expression was assessed on $CD45^+$ cells, $FAP^+$ CAFs, and tumor cells.

Figure S3

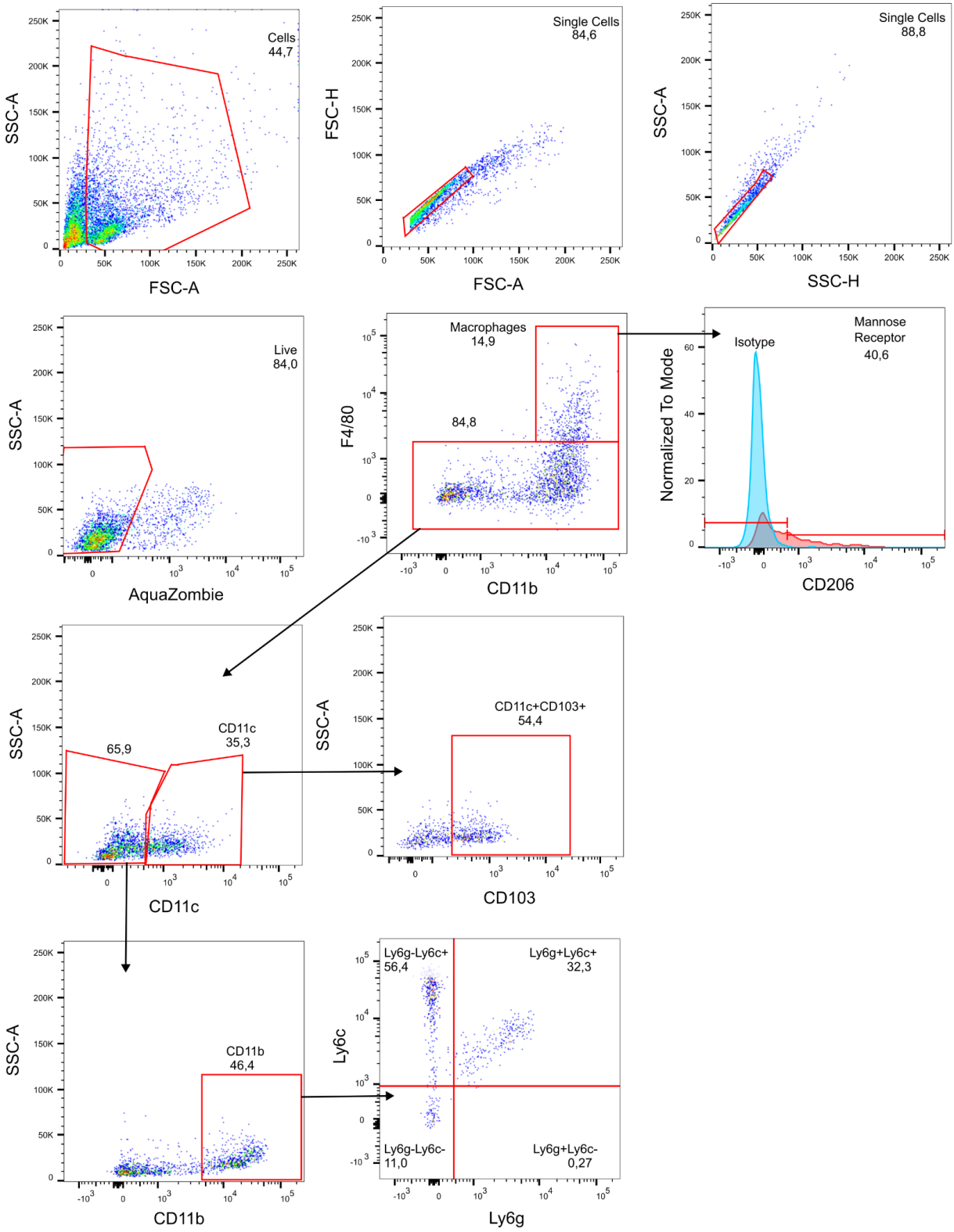


**Figure S3:**

**Gating strategy for myeloid panel.** Representative plots from flow cytometry analysis showing the gating strategy for identification of the indicated cell populations from a single cell suspension of a LL2 tumor. After exclusion of doublets and dead cells, TAMs ($F4/80^{+}CD11b^{+}$) were identified. Expression of the mannose receptor (CD206) was assessed on TAMs. Dendritic cells ($F4/80^{-}CD11c^{+}$) were identified and from this population $CD103^{+}$ dendritic cells were identified. M-MDSCs were identified as being $CD11b^{+}F4/80^{-}Ly6C^{hi}$ and PMN-MDSCs as being $CD11b^{+}F4/80^{-}Ly6C^{lo}Ly6G^{+}$.

Figure S4

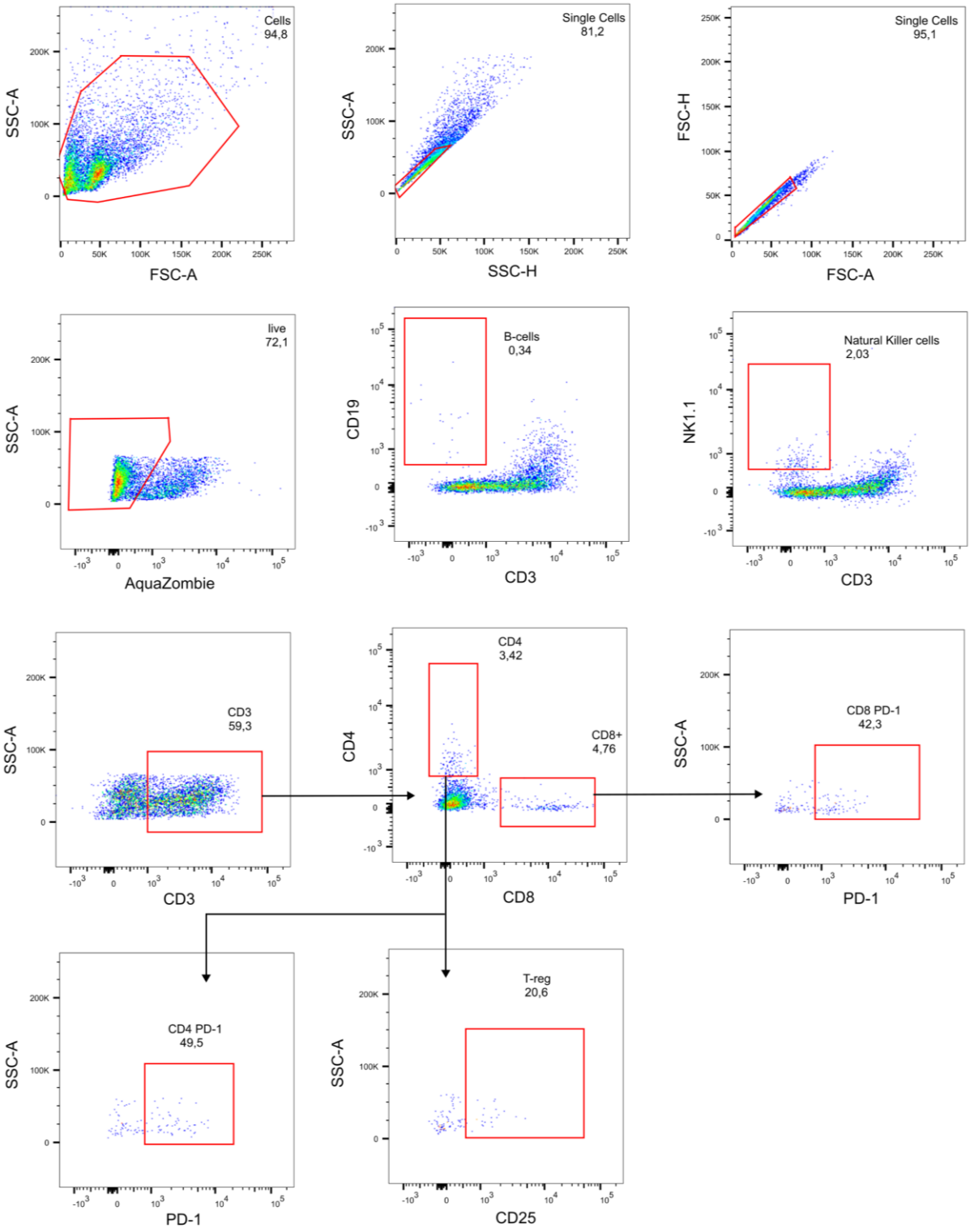


**Figure S4:**

**Gating strategy for lymphoid panel.** Representative plots from flow cytometry analysis showing the gating strategy for identification of the indicated cell populations from a single cell suspension of a LL2 tumor. After exclusion of doublets and dead cells, B cell and NK cells were identified as being $CD3^{-}CD19^{+}$ and $CD3^{-}NK1.1^{+}$, respectively. From the $CD3^{+}$ population, $CD4^{+}$ and $CD8^{+}$ T cells were identified. Within the $CD4^{+}$ populations, $T_{regs}$ ($CD4^{+}CD25^{+}$) were identified. Expression of PD-1 was assessed on $CD4^{+}$ and $CD8^{+}$ T cells.

**Figure S5**

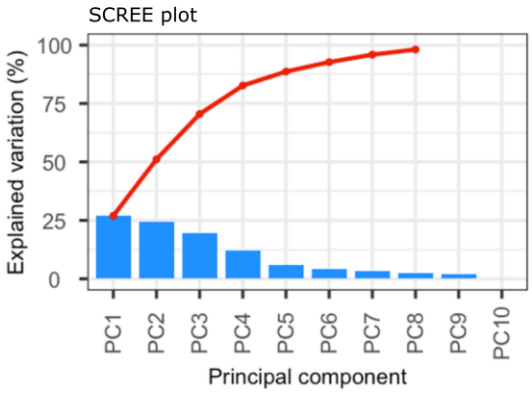


**Figure S5:**

**SCREE plot describing the variability between samples.** The SCREE plot analysis was based on sequenced RNA from FACS-sorted FAP$^{+}$ CAFs.

**Figure S6**

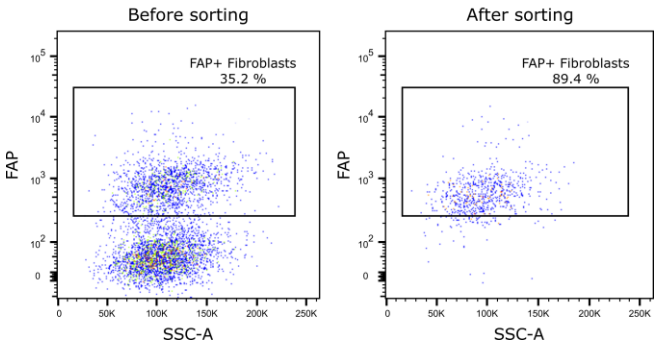


**Figure S6:**

**Sorting efficiency of FAP$^+$ fibroblasts.** Representative dot plots from FACS showing the gating and efficiency of sorting. Sorting was performed after enrichment of CD45$^-$ cells from a single-cell suspension of tumors. Prior to gating for FAP, debris, doublets, and dead cells were excluded.